Cell Death and Differentiation (2004) 11, 618–630

www.nature.com/cdd

RAIDD aggregation facilitates apoptotic death of PC12 cells and sympathetic neurons

O Jabado[1,4], Q Wang[1,4], HJ Rideout[1], M Yeasmin[1], KX Guo[1], K Vekrellis[2], S Papantonis[1], JM Angelastro[3], CM Troy[1,3], L Stefanis*[,1,2,3]

[1] Department of Neurology, Columbia University, USA;
[2] Laboratory of Neurobiology, Institute of Biomedical Research of the Academy of Athens, Athens, Greece;
[3] Department of Pathology, Columbia University, USA
[4] Both these authors have contributed equally to this work
* Corresponding author: L Stefanis, Laboratory of Neurobiology, Institute of Biomedical Research of the Academy of Athens, Soranou Efesiou 4, Papagou 11527, Athens, Greece. Tel: +30-210-6597214; Fax: +30-210-6597545; E-mail: ls76@columbia.edu

Received 15.4.03; revised 24.10.03; accepted 24.11.03; published online 06.2.04
Edited by Dr P Nicotera

Abstract

In human cell lines, the caspase 2 adaptor RAIDD interacts selectively with caspase 2 through its caspase recruitment domain (CARD) and leads to caspase 2-dependent death. Whether RAIDD induces such effects in neuronal cells is unknown. We have previously shown that caspase 2 is essential for apoptosis of trophic factor-deprived PC12 cells and rat sympathetic neurons. We report here that rat RAIDD, cloned from PC12 cells, interacts with rat caspase 2 CARD. RAIDD overexpression induced caspase 2 CARD- and caspase 9-dependent apoptosis of PC12 cells and sympathetic neurons. Apoptosis correlated with the formation of discrete perinuclear aggregates. Both death and aggregates required the expression of full-length RAIDD. Such aggregates may enable more effective activation of caspase 2 through close proximity. Following trophic deprivation, RAIDD overexpression increased death and aggregate formation. Therefore, RAIDD aggregation is important for its death-promoting effects and may play a role in trophic factor withdrawal-induced neuronal apoptosis.

Cell Death and Differentiation (2004) **11,** 618–630.
doi:10.1038/sj.cdd.4401397
Published online 6 February 2004

Keywords: caspase; neuronal death; caspase recruitment domain; PC12 cells; sympathetic neurons; aggregate

Abbreviations: AA, amino acid; Ab, antibody; CARD, caspase recruitment domain; DD, death domain; DED, death effector domain; MTOC, microtubule organizing center; NMR, nuclear magnetic resonance; ORF, open-reading frame; WT, wild type

Introduction

Neuronal apoptotic cell death may play a role in a number of neurological, in particular neurodegenerative, diseases.[1,2] Caspases are cysteine-aspartate proteases that act as participants and executioners of apoptotic cell death pathways. In all, 13 members of this family of proteases have been identified to date.[1,3] All caspases are synthesized as inactive precursors, and generally need to be processed at particular aspartate residues in order to assume an active enzymatic conformation as dimers. Various means of classification of caspases into different subcategories have been proposed. Caspases that possess an approximately 18 kDa N-terminal region, which does not form part of the active enzymatic dimer, are classified as 'prodomain-containing' caspases. A number of these prodomains have been found to interact through their caspase recruitment domains (CARDs) with adaptor molecules, and thus lead to autoactivation of the respective caspases through a close proximity type of interaction. It is thought that these caspases act, for the most part, as 'initiators' of cell death pathways, through subsequent processing and activation of downstream 'effector' caspases, such as caspase 3, or through processing and activation of molecules that lead to the engagement of mitochondrial factors in the apoptotic cascade.[2,3] Among prodomain-containing caspases, however, caspase 2 has been somewhat of an enigma. In various settings it has been found to be processed by caspase 3, situating it at a downstream point in the apoptotic pathway.[4–7] On the other hand, caspase 2 interacts through its prodomain with the adaptor molecules RAIDD/CRADD and ARC,[8–11] is processed early in certain apoptotic pathways[12] and upon overexpression activates the caspase 9/3 cascade.[13,14] More recent studies have suggested that caspase 2 acts upstream of cytochrome *c* release.[14–17] The particular position of caspase 2 within apoptotic cascades is therefore unclear, and may differ depending on the apoptotic stimulus and cell type.

We and others have previously shown that caspase 2 is essential for trophic factor deprivation-induced death of PC12 cells and sympathetic neurons.[18–21] Caspase 2 processing occurs at the same time point as caspase 3-like activation in serum-deprived PC12 cells, and complete inhibition of caspase 3-like activity does not prevent caspase 2 processing.[20,22] This suggests that, in this model, caspase 2 processing occurs in a manner independent of caspase 3. Therefore, other mechanisms for caspase 2 processing and activation need to be invoked in this apoptotic pathway.

In this paper, we have focused on the caspase 2 adaptor RAIDD/CRADD, which has been shown to interact selectively with caspase 2 and to induce apoptosis upon overexpression in non-neuronal cells.[8,9] We have cloned rat RAIDD from PC12 cells and have examined the effects of overexpression of various forms of this molecule in PC12 cells and in sympathetic neurons. Our results show for the first time that RAIDD-induced apoptotic death of neuronal cells correlates with the formation of cytoplasmic perinuclear aggregates. These aggregates may facilitate the activation of caspase 2 through close proximity.

Results

Cloning of rat RAIDD from PC12 cells

Rat RAIDD, cloned by RACE, had a high degree of homology at the AA level with mouse (Accession #AJ224738) and human (Accession #U79115) RAIDD/CRADD. Identity with mouse/human RAIDD was 94 and 90%, and similarity 97 and 94%, respectively. Homology with human RAIDD is shown in Figure 1a. Particularly striking is the degree of conservation within the shaded N-terminal CARD region (as defined by nuclear magnetic resonance (NMR), Chou *et al*.[23]). Within this region, there is a high degree of homology with the N-terminal CARD of rat caspase 2.[20] For the sequence spanning residues 4–93 of rat RAIDD, which defines the six helices of the RAIDD CARD,[23] there is 54.4% similarity and 28.9% identity with rat caspase 2 (Figure 1b).

Interaction between various RAIDD and caspase 2 constructs upon overexpression in 293T cells

To evaluate specific functional domains of rat RAIDD and caspase 2 and interactions between them, we generated a number of mutated or truncated constructs of these two molecules. The constructs utilized are depicted in Figure 2. These include: RAIDDM, identical to wild-type (WT) RAIDD, except for mutation L27F, which has previously been shown to prevent the interaction between human RAIDD and caspase 2 CARDs;[8] RAIDD(1–83), encoding residues 1–83 of WT RAIDD, thus encompassing the initially identified area of homology with caspase 2 CARD;[8] RAIDD(1–117), encoding residues 1–117 of WT RAIDD, thus encompassing the full six-helical loop of the CARD, as defined by NMR;[23] RAIDD(DD), encoding residues 115–199, thus containing the death

a

```
Rat:     1 MDARDKQVLRSLRLELGAEVLVEGLVLQYL 30
           M+ARDKQVLRSLRLELGAEVLVEGLVLQYL
Human:   1 MEARDKQVLRSLRLELGAEVLVEGLVLQYL 30

Rat:    31 YQEGILTENHIQEIKAQTTGLRKTMLLLDI 60
           YQEGILTENHIQEI AQTTGLRKTMLLLDI
Human:  31 YQEGILTENHIQEI NAQTTGLRKTMLLLDI 60

Rat:    61 LPSRGPKAFDTFLDSLQEFPWVREKLEKAREEA 93
           LPSRGPKAFDTFLDSLQEFPWVREKL+ KAREEA
Human:  61 LPSRGPKAFDTFLDSLQEFPWVREKLKKAREEA 93

Rat:    94 TA ELP T GDWMSGIPSHILNSSPSDRQI 120
              + LP  GD  ++ GIPSHILNSSPSDRQI
Human:  94 MTDLP A GD R LT GIPSHILNSSPSDRQI 120

Rat:   121 NQLAQKLGPEWEPMVLSLGLSQTDIYRCKA 150
           NQLAQ+LGPEWEPMVLSLGLSQTDIYRCKA
Human: 121 NQLAQRLGPEWEPMVLSLGLSQTDIYRCKA 150

Rat:   151 NHPHNVQSQVVEAFVRWRQR Y GKQATFLSL 180
           NHPHNVQSQVVEAF+RWRQR + GKQATF  SL
Human: 151 NHPHNVQSQVVEAFI RWRQR F GKQATFQSL 180

Rat:   181 HKGFQAVEADPSLLQHMLE 199
           H  G  +AVE  DPSLL  HMLE
Human: 181 HNGLRAVEVDPSLLL HMLE 199
```

b

```
Rat RAIDD 4   RDK QVLRSLRLELGAEVLVEG LV L QYLYQEGILTENHI QEI 44
                + +  L+    R+ L    + +L+     L  L ++ L  ++   I+T       + I
Rat Cas2  35 DHQE TLKKNRVVLAKQLLLSE  L- LEH LLEKD I ITLEMRELI 74

 45 KAQTTGLRK TMLLLDI LPSRGPKAFDTF LDSLQEFPWVR EKLEKAREEA 93
    +A +         +  +  LL++LP  RGP+AFD   F  ++L+ E             LE
 75 QAKGGSFSQNVELLNLLPKRGPQAFDAFCEALRETRQGH - - LED LLLTT 121
```

Figure 1 Diagram of homology between rat and human RAIDD. The sequence of rat RAIDD is compared to the reported sequence of human RAIDD/CRADD.[8,9] Nonconservative substitutions are highlighted in bold and larger font. Conservative substitutions are indicated by crosses. (**b**). Diagram of homology between the CARDs of rat caspase 2 and rat RAIDD. The CARD, as defined by Chou *et al*.[23] of rat RAIDD is compared to the CARD of rat caspase 2.[20] The middle row indicates common AAs or conservative substitutions. The leucine (L) residue highlighted at position 27 of rat RAIDD is highly conserved, and when mutated leads to a loss of interaction between the CARDs of human RAIDD and caspase 2[8]

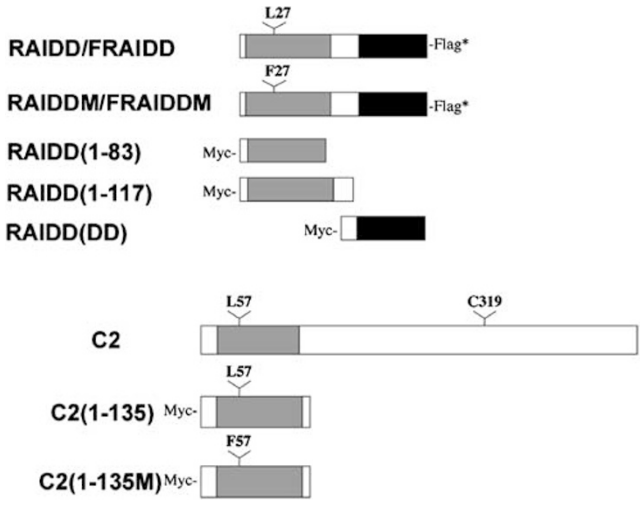

Figure 2 Rat RAIDD and caspase 2 constructs utilized. The gray areas denote CARDs. The black area in RAIDD denotes the DD. L27 in RAIDD and L57 in caspase 2 are critical residues for CARD interaction.[8] C319 represents the catalytic cysteine on caspase 2. The asterisk on the Flag tag in the RAIDD and RAIDDM constructs indicates that constructs were generated both with and without the Flag tag

domain (DD);[8,9] C2(1–135), encoding residues 1–135 of rat caspase 2, thus encompassing the CARD, but without containing the full prodomain; C2(1–135M), identical to C2(1–135), except for mutation L57F, which corresponds to residue L27 of RAIDD (see Figure 1b), and has previously been shown to prevent the interaction between human RAIDD and caspase 2 CARDs.[8] All these constructs were Myc tagged, except for RAIDD and RAIDDM, which were either untagged or Flag tagged.

We first evaluated the interaction between RAIDD and C2(1–135) or C2(1–135M) by cotransfecting them in 293T cells, which have the advantage of higher transfection efficiency. Flag-tagged RAIDD co-immunoprecipitated Myc-tagged C2(1–135), but not C2(1–135 M) (Figure a), consistent with the results of Duan and Dixit.[8] We then evaluated whether RAIDDM interacted with C2(1–135). Flag-tagged RAIDDM also co-immunoprecipitated Myc-tagged C2(1–135) (Figure 3b), in apparent contradiction to the results of Duan and Dixit.[8] This suggests that the full-length RAIDDM, as opposed to the CARD-containing-only RAIDDM that was used by Duan and Dixit,[8] may assume a different conformation, which allows it to interact with the caspase 2 CARD even in the presence of the L27F mutation. We also performed immunoprecipitation with the Flag antibody (Ab) after the overexpression of Flag-tagged caspase 9 DN and RAIDD. No specific labeling was seen when the blots were probed for RAIDD (data not shown), indicating that, as reported previously,[8] there is no physical association between RAIDD and caspase 9.

We conclude that previously observed interactions between the CARDs of human caspase 2 and RAIDD also occur within cells upon overexpression of the rat homologues. However, the specificity of such interactions may be altered in the context of the full-length RAIDD molecule.

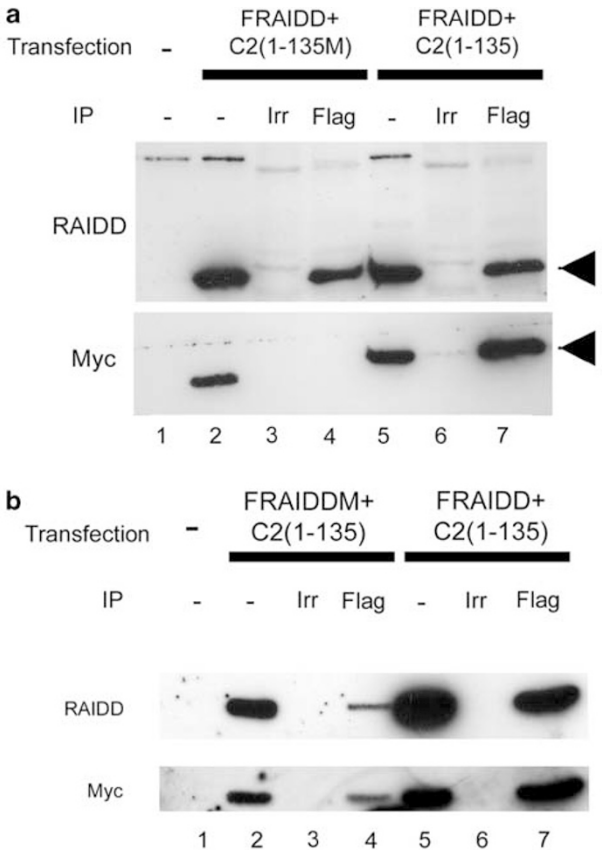

Figure 3 Interactions between rat RAIDD and caspase 2 constructs upon overexpression in 293T cells. (**a**) 293T cells were cotransfected with Flag-tagged RAIDD (FRAIDD) and Myc-tagged C2(1–135) or C2(1–135 M) in equimolar ratios. After 24 h, the cells were lysed and immunoprecipitation was performed with Flag Ab or GAPDH Ab, as an irrelevant (Irr) control (1 μg/ml). Following rinses, eluted material from original 500 μg protein was run on 12% SDS-PAGE gels and immunoblotted with RAIDD (top) or Myc (bottom panel) Abs. Lanes 1, 2 and 5 represent lysates (10 μg) of 293T cells, nontransfected [1] or transfected.[2,5] Arrowheads denote immunoreactive bands for RAIDD in the upper and Myc in the bottom panel. Note that RAIDD is immunoprecipitated in both cases (top panel), whereas only C2(1–135), but not C2(1–135 M), co-immunoprecipitates (bottom panel, compare lane 7 with lane 4). (**b**) 293T cells were cotransfected with Flag-tagged RAIDD or RAIDDM and Myc-tagged C2(1–135) in equimolar ratios. Immunoprecipitations were performed as above with Flag or GAPDH Abs and Western immunoblots were performed with RAIDD (top) or Myc Abs (bottom panel). The first, second and fifth lanes again denote cell lysates. In both cases, Myc-tagged C2(1–135) co-immunoprecipitates RAIDD (lanes 4 and 7). Even though the transfection efficiency is higher for RAIDD, the ratio of immunoprecipitated C2(1–135) to RAIDD is equal between the IPs

RAIDD-induced perinuclear aggregate formation

We then analyzed the immunostaining pattern of overexpressed full-length RAIDD in PC12 cells and sympathetic neurons (Figure 4a and b). Cells overexpressing RAIDD were identified by a commercial polyclonal Ab raised against an epitope spanning amino acids (AA) 112–126 of human RAIDD (StressGen). When the pCMS-EGFP vector was used for overexpression, RAIDD immunostaining of PC12 cells and sympathetic neurons was intense only in cells that were also EGFP positive (for example, see Figure 4b). The same RAIDD Ab recognized the expected 23 kDa band upon overexpression of rat RAIDD in PC12 cells (Figure 4c). In conjunction, these data indicate that this Ab recognizes

specifically and reliably overexpressed rat RAIDD. Substantially lower levels of endogenous RAIDD were seen by immunostaining of nontransfected PC12 cells or sympathetic neurons and by Western immunoblot of lysates of untransfected PC12 cells (data not shown).

In a percentage of transfected PC12 cells or sympathetic neurons, overexpressed RAIDD localized predominantly within a discrete focal perinuclear cytoplasmic region (Figure 4a, b and d–f). These 'aggregates' typically had a spherical shape (Figure 4a, b and d), and their perinuclear location was clearly demonstrated by confocal microscopy (Figure 4d). Human Flag-tagged RAIDD (FhRAIDD) also formed such perinuclear aggregates, and these were identified both by RAIDD and Flag immunostaining (see). RAIDD-overexpressing cells that did not show focal aggregation demonstrated an intense immunostaining pattern throughout the cell body (data not shown).

In contrast to the effects seen with RAIDD overexpression, RAIDDM showed a more diffuse pattern of immunostaining and fewer aggregates in PC12 cells and sympathetic neurons (Figure 4a, e and f). Flag-tagged rat RAIDD (FRAIDD) induced aggregates to a similar low extent as untagged RAIDDM in PC12 cells, but in sympathetic neurons aggregates were more numerous (Figure 4e and f). Of note, such differences were not related to expression levels, because the intensity of RAIDD immunostaining in single cells was similar across the constructs utilized (see Figure 4a).

To examine which region of RAIDD is required for the formation of the perinuclear aggregates, we also overexpressed truncated versions of RAIDD. Neither CARD-containing constructs (RAIDD(1–83) or RAIDD(1–117) nor DD-containing constructs (RAIDD(DD)) induced aggregates (data not shown), suggesting that the full-length RAIDD is required for their formation.

The perinuclear localization of RAIDD-induced aggregates suggested Golgi localization, which has previously been reported for endogenous caspase 2.[24] Double immunostain-

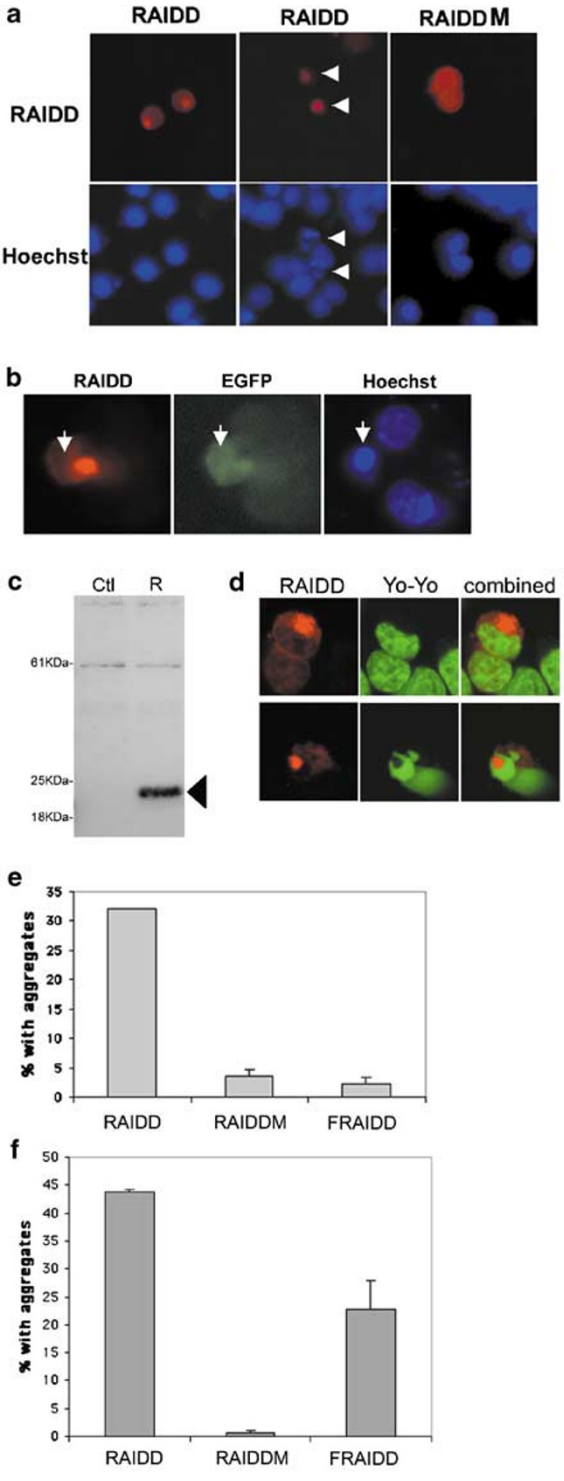

Figure 4 Formation of aggregates upon overexpression of rat RAIDD. (**a**) PC12 cells were transfected with pCMS-EGFP vectors encoding RAIDD (left and central panel) or RAIDDM (right panel). After 48 h, cells were fixed and immunostained with RAIDD Ab and labeled with Hoechst. Representative indirect immunofluorescence images of RAIDD-overexpressing cells are shown. Note the focal, discrete pattern of RAIDD immunostaining in RAIDD-overexpressing cells, compared to the diffuse pattern in RAIDDM-overexpressing cells. Note also that the two RAIDD-overexpressing cells in the middle panel show apoptotic morphology by Hoechst (arrow heads). (**b**) Sympathetic neurons were transfected with a pCMS-EGFP vector encoding RAIDD. After 60 h, cells were fixed and immunostained with a RAIDD Ab and labeled with Hoechst. A representative indirect immunofluorescence image of an EGFP/RAIDD-overexpressing neuron with a RAIDD aggregate and nuclear apoptotic morphology is shown. The position of the apoptotic nucleus is depicted by an arrow. Two other nontransfected neurons show normal nuclear morphology. (**c**) PC12 cells were transfected with EGFP alone (ctl) or together with RAIDD (R). After 36 h, the cells were lysed and the samples were analyzed by Western immunoblotting using RAIDD Ab. The arrow head depicts the overexpressed 23 kDa rat RAIDD. (**d**) PC12 cells were transfected with a pCDNA3 vector encoding RAIDD. Cells were fixed and stained with the RAIDD Ab and the nuclear dye Yo-Yo and visualized by confocal microscopy. All RAIDD aggregates identified by confocal microscopy clearly lay outside the nucleus, in a perinuclear location. Representative images of a nonapoptotic (top) and an apoptotic (bottom) cell that demonstrate RAIDD aggregates are shown. (**e** and **f**). PC12 cells (**e**) or neonatal rat sympathetic neurons (**f**) were transfected with pCMS-EGFP vectors encoding RAIDD, RAIDDM or FRAIDD. After 48 h, cells were fixed and immunostained with Abs directed against RAIDD. The results are reported as mean $\pm$ S.E.M. ($n=3$). RAIDD-expressing PC12 cells were significantly more likely to demonstrate aggregates compared to RAIDDM- or FRAIDD-expressing cells ($P<0.0001$, ANOVA). RAIDD-expressing sympathetic neurons were significantly more likely to demonstrate aggregates compared to RAIDDM- or FRAIDD-expressing neurons ($P<0.01$ *versus* FRAIDD and $P<10^{-6}$ *versus* RAIDDM, ANOVA). This is representative of four (PC12 cells) and two (sympathetic neurons) independent experiments

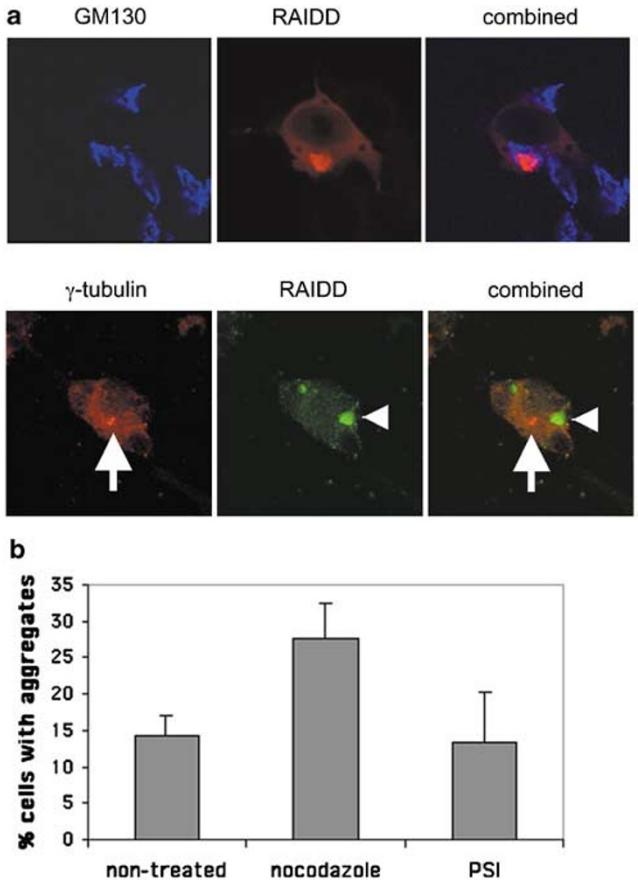

Figure 5 RAIDD overexpression-induced aggregates/oligomers do not localize to the Golgi and are not aggresomes. (**a**). PC12 cells were transfected with a pCMS-EGFP (top panel) or a PCDNA3 vector (bottom panel) encoding RAIDD. After 36 h, cells were fixed and immunostained with RAIDD Ab (middle panel) and a monoclonal GM130 Ab to label the Golgi apparatus (top left panel) or a monoclonal γ-tubulin Ab to label the MTOC (bottom left pannel, Johnston *et al*.[25]). Secondary antibodies used were Cy3 anti-rabbit and Cy5 anti-mouse (top), or Cy2 anti-rabbit and Cy3 anti-mouse (bottom). Cells were then visualized under a confocal microscope. Representative images are shown, with combined images on the right. Note the lack of colocalization between RAIDD aggregates and GM130 or γ-tubulin. The arrow depicts the MTOC and the arrow head a RAIDD aggregate. (**b**) PC12 cells were transfected with a pCMS-EGFP vector encoding RAIDD. After 24 h, the cell culture medium was replaced with complete medium without additives (nontreated), or containing 5 μM PSI or 10 μg/ml nocodazole. After 7 h, the cells were fixed and immunostained for RAIDD and labeled with Hoechst. The percentage of cells bearing aggregates was assessed in each condition by indirect immunofluorescence

ing with a Golgi marker, GM130, however, and visualization by confocal microscopy revealed close apposition, but not colocalization (Figure 5a). The perinuclear localization also raised the possibility of an 'aggresome', an inclusion formed in the microtubule organizing center (MTOC) of cells upon overexpression of misfolded proteins, such as CFTR.[25] However, using confocal microscopy, we found little colocalization between the MTOC marker γ-tubulin and RAIDD-induced aggregates (Figure 5a). Furthermore, there was no increase in the number of cells with RAIDD-induced aggregates upon treatment with the proteasomal inhibitor PSI, or inhibition upon treatment with the microtubule destabilizer nocodazole (Figure 5b), as has been reported for aggresomes.[25]

We conclude that the full-length rat RAIDD aggregates in perinuclear regions of PC12 cells and sympathetic neurons. The formation of these aggregates is disrupted by the L27F mutation, and, less so, and depending on the cellular context, by the presence of a Flag tag.

Insolubility of RAIDD aggregates

To further investigate the nature of the RAIDD-induced aggregates, we transfected PC12 cells with rat RAIDD or RAIDDM, and 48 h later exposed the cultures to a brief period of detergent extraction, as we have described previously.[26] This procedure extracts the soluble components of the cytoplasm, and only relatively insoluble or filamentous cytoplasmic material remains. Following this procedure, the cells were fixed and analyzed for RAIDD immunostaining. Both the low-level endogenous RAIDD immunostaining and the diffuse immunostaining of overexpressed RAIDD were abolished. In contrast, the discrete, focal, perinuclear immunostaining pattern of overexpressed WT RAIDD was still apparent (Figure 6a). This indicates that RAIDD within these aggregates has a conformation that renders it resistant to detergent extraction.

To analyze further at the biochemical level this form of overexpressed RAIDD, we turned to SH-SY5Y neuroblastoma cells, because the higher transfection efficiency in these neuronal cultures enables more detailed biochemical analysis. We first verified that overexpression of the various forms of RAIDD in these cells reproduced the formation of aggregates, as seen in PC12 cells (data not shown). We then performed Western immunoblots of lysates of these cells that had been transfected with two constructs that induced a substantial number of aggregates (rat RAIDD, human Flag-tagged RAIDD (FhRAIDD)) or two that did so to a much lesser extent (Flag-tagged rat RAIDDM (FRAIDDM) and Flag-tagged rat RAIDD (FRAIDD)). We separated the lysates in detergent soluble and insoluble, as described previously,[26] so as to focus our attention to the pool of RAIDD that is relatively insoluble. Although the levels of the various forms of RAIDD in the detergent-soluble fraction were similar (Figure 6b), there was a marked increase in detergent-insoluble RAIDD in the cells expressing rat RAIDD or hFRAIDD (Figure 6c). Furthermore, an increase in higher molecular weight forms of RAIDD, including forms that did not leave the stacking gel, was seen almost exclusively in these lysates (Figure 6c).

In conjunction, these results are consistent with the idea that detergent-insoluble RAIDD accumulates in these aggregates.

Apoptosis induced by the overexpression of RAIDD in PC12 cells and sympathetic neurons

We then examined whether RAIDD overexpression in PC12 cells induces apoptotic death, as previously reported for its human homologue in other cell types.[8,9,14] Overexpression of WT rat RAIDD induced apoptotic death, albeit variable from experiment to experiment and of lower magnitude compared to previous studies[8,9] (Figure 7a and b). The reason for this variability is unclear, but may relate to the baseline death in

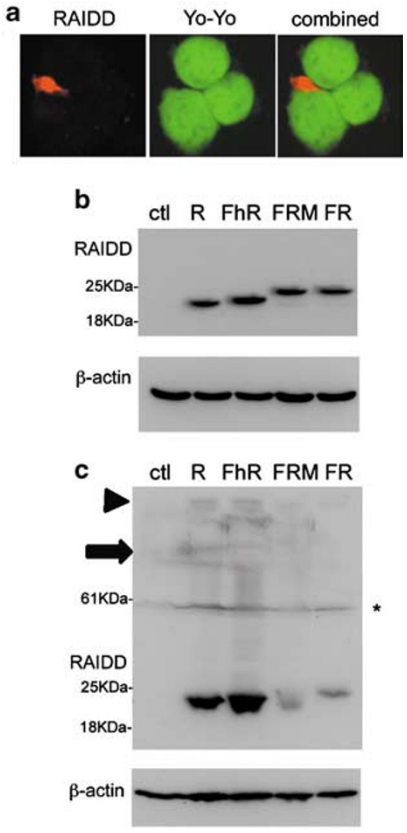

Figure 6 RAIDD-induced aggregates are relatively insoluble. (**a**) PC12 cells were transfected with RAIDD, and 2 days later exposed to a detergent buffer for 10 min, as described.[26,33] The cells were then fixed and immunostained for RAIDD and labeled with Yo-Yo. A representative confocal image is shown, demonstrating the preservation of RAIDD-induced aggregates, whereas the diffuse RAIDD immunostaining is lost. (**b** and **c**). SH-SY5Y neuroblastoma cells were transfected with EGFP (ctl), RAIDD (R), human Flag-tagged RAIDD (FhRAIDD, FhR), Flag-tagged RAIDDM (FRM) or Flag-tagged RAIDD (FR). After 2 days, cells were lysed and separated in detergent-soluble (**b**) and detergent-insoluble components (**c**). These were run on SDS/PAGE gels and immunoblotted with anti-RAIDD. Blots were then stripped and immunoblotted with anti-β-actin. In (**b**), similar amounts of detergent-soluble RAIDD were expressed with the different constructs. Detergent-insoluble RAIDD, however, was substantially higher in cells expressing RAIDD or FhRAIDD (**c**). The arrow depicts the end of the stacking gel. The arrow head depicts bands at the top of the stacking gel in RAIDD- and FhRAIDD-expressing cell lysates. The asterisk depicts what is likely a nonspecific band at 60 kDa

the cultures (compare apoptosis in EGFP-expressing cells in Figure 7a with that in Figure 7b). Overexpression of Flag-tagged human RAIDD (FhRAIDD),[27] kindly provided to us by Drs. Kumar and Shearwin-Whyatt (Adelaide, Australia), induced a similar magnitude of apoptosis in PC12 cells (data not shown). Interestingly, overexpression of RAIDDM or Flag-tagged rat RAIDD (FRAIDD) induced less apoptotic death (Figure 7a and b). We had similar findings in sympathetic neurons, although in this case FRAIDD induced only slightly lower extent of death compared to RAIDD (Figure 7c). Consistent with the need for an association with the caspase 2 CARD for death induction, coexpression of the CARD-containing C2(1–135), which presumably acted as a dominant negative by preventing the interaction of overexpressed RAIDD with endogenous caspase 2, inhibited RAIDD-induced death (Figure 7d). Another caspase 2 DN construct, containing a mutation in the catalytic site, also prevented RAIDD-induced apoptosis (data not shown). This death could also be inhibited by the general caspase inhibitor BAF (Figure 7b) or by the coexpression of caspase 9 DN (C9DN, Figure 7d). Expression of truncated forms of rat RAIDD (RAIDD1-83), RAIDD(1–117). RAIDD(DD)) failed to induce apoptosis in PC12 cells or sympathetic neurons (data not shown).

In view of the protective effect of C9DN on RAIDD-induced death, we wished to examine further whether elements of the 'intrinsic' apoptotic pathway were activated following RAIDD overexpression. We first examined whether there was evidence of cytochrome *c* release, a crucial element in such 'intrinsic' apoptotic pathways. We found that some PC12 cells that overexpressed RAIDD showed the loss of mitochondrial cytochrome *c* staining, similar to what has been observed in other models of neuronal apoptosis (e.g. 7). In contrast, cells overexpressing EGFP did not show such loss (Figure 8a). In addition, some PC12 cells overexpressing FhRAIDD, but not those overexpressing EGFP, showed activation of caspase 3, determined by immunostaining with an Ab that specifically recognizes activated caspase 3 (Figure 8b). Such results are in agreement with the results of Guo *et al*.,[14] who showed the activation of elements of the 'intrinsic' apoptotic pathway following human RAIDD overexpression in non-neuronal cells.

We conclude that the full-length rat RAIDD overexpression induces apoptotic death of PC12 cells and sympathetic neurons. An association with the caspase 2 CARD is necessary to induce death, because apoptosis is inhibited by the coexpression of a DN form of caspase 2 containing only the CARD. RAIDD-induced death is also dependent on the activation of the caspase 9/3 pathway.

Relationship between RAIDD aggregation and cell death

Given the induction of RAIDD aggregation and cell death upon rat RAIDD or FhRAIDD overexpression, and the relative lack of either of these phenomena upon RAIDDM or FRAIDD overexpression, we hypothesized that RAIDD aggregation may be contributing to death. Consistent with this idea, most cells that showed morphological or biochemical evidence of activation of apoptotic pathways expressed RAIDD in an aggregated conformation (see Figures 4 and 8). To look at this correlation in a more quantitative manner, we counted the percentage of PC12 cells overexpressing nonaggregated or aggregated RAIDD that were apoptotic at baseline, and then following serum deprivation. We found that in control cultures PC12 cells expressing RAIDD in an aggregated conformation were 3–4 times more likely to be apoptotic compared to those that showed diffuse RAIDD immunostaining. When cultures were serum deprived, there was further marked potentiation of death in the aggregate-bearing cells (Figure 9a). Overall, there was a 50% potentiation of serum deprivation-induced death in RAIDD- compared to EGFP-expressing cells (17.7% serum deprivation-induced apoptosis in EGFP-expressing cells *versus* 26.4% in RAIDD-expressing cells) (Figure 9a). Interestingly, the percentage of RAIDD-expressing cells

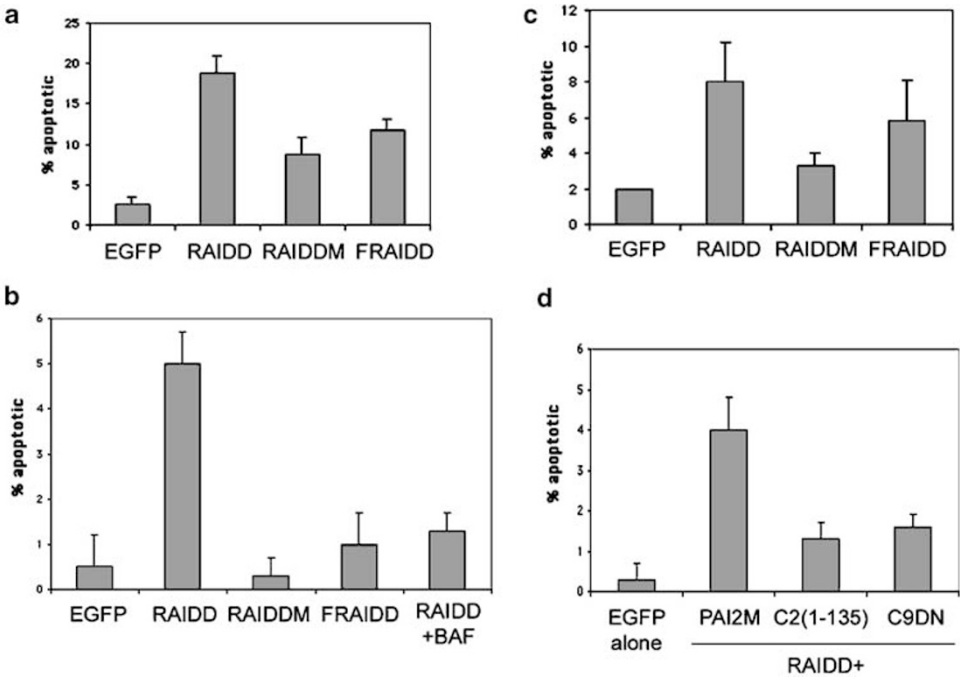

Figure 7 RAIDD overexpression induces apoptosis that is dependent on interaction with the caspase 2 CARD and on caspase 9. (**a** and **b**). PC12 cells were transfected with pCMS-EGFP vectors encoding no additional gene (EGFP), RAIDD, RAIDDM or FRAIDD. After 2 days, the cells were fixed and immunostained with Abs directed against RAIDD and labeled with Hoechst. The percentage of EGFP- or RAIDD-positive cells showing nuclear apoptotic morphology was assessed. (**a**) and (**b**) are representative experiments, and demonstrate the variability in RAIDD-induced apoptosis. Results are reported as mean $\pm$ S.E.M. ($n=3$). In (**a**) and (**b**), RAIDD induced significantly more apoptotic death compared to EGFP, RAIDDM or FRAIDD ($P<0.001$, ANOVA). In (**b**), BAF (50 μM, Enzyme Systems Products), applied at the time of replenishing the medium after transfection, significantly protected against RAIDD-induced death ($P<0.0005$, ANOVA). (**c**) Neonatal rat sympathetic neurons were cultured for 4 days and then were transfected with pCMS-EGFP vectors encoding no additional gene, RAIDD, RAIDDM or FRAIDD. After 2 days, the cells were fixed and immunostained with Abs directed against RAIDD and labeled with Hoechst. Results are reported as mean $\pm$ S.E.M. ($n=4$). RAIDD induced significantly more death compared to EGFP or RAIDDM ($P<0.05$, ANOVA). There was no significant difference between the death induced by FRAIDD and that induced by the other constructs. This is representative of two independent experiments. (**d**) PC12 cells were transfected with a pCMS-EGFP vector encoding EGFP alone or cotransfected, in a 1 : 3 ratio, with a PCDNA3 vector encoding RAIDD and pCMS-EGFP vectors encoding Myc-tagged PAI2MT, Myc-tagged C2(1–135) or Flag-tagged caspase 9 DN (C9DN). After 48 h, the cells were fixed and immunostained for Myc (RAIDD + PAI2MT and RAIDD + C2(1–135)) or Flag (RAIDD + C9DN) and labeled with Hoechst. The percentage of EGFP (for EGFP alone), Myc (for RAIDD + PAI2MT and RAIDD + C2(1–135)) and Flag (for RAIDD + C9DN)-positive cells that showed features of nuclear apoptosis was assessed. Results are reported as mean $\pm$ S.E.M. ($n=3$). There was significantly more apoptosis in cells expressing PAI2MT compared to all other conditions ($P<0.05$, ANOVA)

bearing aggregates increased about 50% following serum deprivation (Figure 9a).

To examine whether the formation of aggregates was a late event in RAIDD-induced death, which was rather an effect of the cellular shrinkage and other alterations that occur in apoptosis, or whether it represented an earlier event with a potential causal role in apoptosis, we performed similar experiments in the presence of the caspase inhibitor BAF. We reasoned that if BAF prevented the formation of aggregates, these would be a late event in apoptosis, whereas, if it did not, this would imply that they occurred early in RAIDD-induced apoptosis. We found that RAIDD overexpression in the presence of BAF led to an increase in the percentage of cells bearing aggregates, compared to those cultures where RAIDD overexpression was performed in the absence of additives (Figure 9b). There was a further marked increase of cells bearing aggregates following serum deprivation in the presence of BAF. Again, as in Figure 9a, there was a substantial increase of aggregation with serum deprivation alone compared to the control state (Figure 9b). The increase of aggregate formation in BAF-treated cultures is likely due to the fact that cells accumulating aggregates, which would normally undergo subsequent apoptosis, do not do so in the presence of caspase inhibition, and thus accumulate in the cultures.

These results support the idea that aggregation of RAIDD is, at least in part, responsible for its death-promoting effects in PC12 cells and sympathetic neurons. They further raise the possibility that some form of RAIDD aggregation may occur physiologically with trophic deprivation, because, following this stimulus, such aggregates increased substantially.

Discussion

In the current paper, we have examined the role of the caspase 2 interactor RAIDD in mediating PC12 cell and sympathetic neuron apoptosis. As reported in previous studies with human RAIDD,[8,9] the rat homologue induces apoptosis in these cell culture systems. In agreement with a more recent study,[14] overexpression of RAIDD appears to activate the mitochondrial pathway of apoptosis, as evidenced by cytochrome *c* release, caspase 3 activation and inhibition of death by DN caspase 9 or a general pharmacological

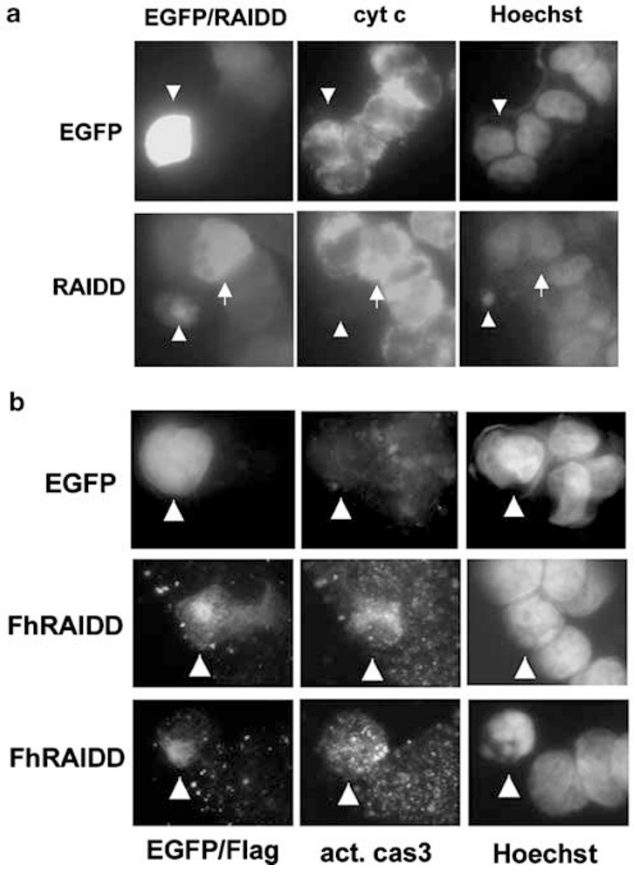

Figure 8 RAIDD overexpression induces loss of mitochondrial cytochrome *c* and caspase 3 activation. (**a**) A pCMS-EGFP vector encoding EGFP alone or a PCDNA3 vector encoding RAIDD were transfected into PC12 cells. After 48 h, the cells were fixed and immunostained for cytochrome *c* alone (top panel) or for RAIDD and cytochrome *c* (bottom panel) and counterstained with Hoechst. A cell overexpressing RAIDD in an aggregated conformation (left panel, depicted by an arrow head) that has lost cytochrome *c* staining (middle panel) and shows nuclear apoptosis (right panel), and another cell with diffuse RAIDD immunostaining without the loss of cytochrome *c* staining or apoptotic morphology (arrow) are shown in the bottom panel. As a control, a representative image of an EGFP-overexpressing cell with maintained cytochrome *c* staining (arrow head) is shown in the top panel. (**b**) A pCMS-EGFP vector encoding EGFP alone or a pCNX2 vector encoding Flag-tagged human RAIDD (FhRAIDD) were transfected into PC12 cells. After 48 h, the cells were fixed, immunostained for Flag and the active form of caspase 3 and labeled with Hoechst. Two representative indirect immunofluorescence images of RAIDD-overexpressing cells with positive activated caspase 3 are shown in the middle and lower panel. The cell indicated by the arrow head in the middle panel is nonapoptotic, whereas the one in the lower one is apoptotic. Note the focal perinuclear staining pattern of Flag. A representative image of an EGFP-overexpressing cell (arrow head) showing the absence of activated caspase 3 is shown in the top panel

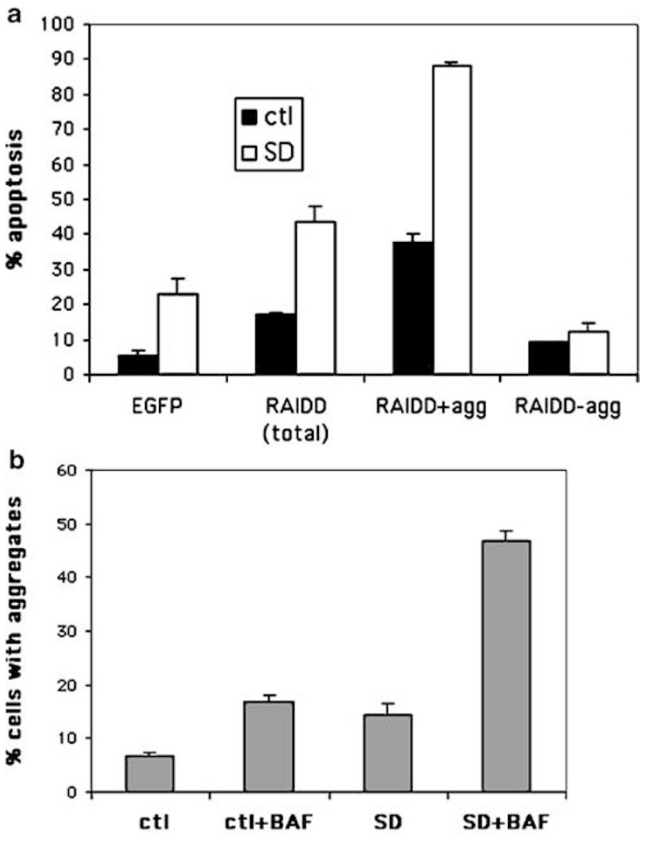

Figure 9 RAIDD-induced aggregate formation facilitates serum deprivation-induced PC12 cell apoptosis. (**a**) PC12 cells were transfected with a pCMS-EGFP vector encoding EGFP alone or, in addition, RAIDD. After 24 h, the cells were either deprived of serum (S.D.) or maintained in serum (ctl). After 24 h, the cells were fixed and immunostained with RAIDD Ab and labeled with Hoechst. More than 300 EGFP- or RAIDD-overexpressing cells were counted in two individual wells for each condition. In the case of RAIDD-expressing cells, these were analyzed, in addition to apoptosis, for the presence or absence of aggregates (agg). The results are reported as mean $\pm$ S.E.M. ($n=2$). RAIDD-expressing cells with aggregates were significantly more likely to be apoptotic compared to those without aggregates, both at baseline and following serum deprivation ($P<0.0005$, ANOVA). Similar results were achieved in three independent experiments. (**b**) PC12 cells were transfected with a pCMS-EGFP vector encoding RAIDD. After 24 h, the cells were either deprived of serum (S.D.) or maintained in serum (ctl) in the presence or absence of BAF. After 24 h, the cells were fixed and immunostained with RAIDD Ab and labeled with Hoechst. More than 150 RAIDD-overexpressing cells were counted in two individual wells for each condition. The results are reported as mean $\pm$S.E.M. ($n=2$). The presence of BAF led to a significant increase in the percentage of cells bearing aggregates both in the serum-containing ($P<0.05$, Student's *t*-test) and serum-deprived state ($P<0.005$, Student's *t*-test). Serum deprivation alone led to a significant increase in aggregate formation compared to the ctl state ($P<0.05$, Student's *t*-test). Similar results were achieved in two independent experiments

caspase inhibitor. In addition, C2(1–135), a truncated form of caspase 2, containing the RAIDD-binding CARD domain, blocked RAIDD-induced apoptotic death. It should be noted that this DN approach is very specific, because the CARD of caspase 2 that comprises this construct has no appreciable homology with other caspases. Therefore, C2(1–135) inhibits only signaling related to caspase 2, and not other caspases, and prevents the association between overexpressed RAIDD and endogenous caspase 2. As RAIDD interacts directly with caspase 2, but not caspase 9, we propose a model in which following RAIDD overexpression there is initial RAIDD/caspase 2 interaction, which can be blocked by the coexpression of C2(1–135). Subsequently, there is the activation of the mitochondrial pathway of apoptosis (see schematic diagram of apoptotic pathway induced by RAIDD overexpression in Figure 10). Such a sequence of events has been recently shown with caspase 2 overexpression.[13,14] We should note that, based on our studies, we cannot exclude the possibility that, in addition to apoptosis, other forms of death occur with RAIDD overexpression.

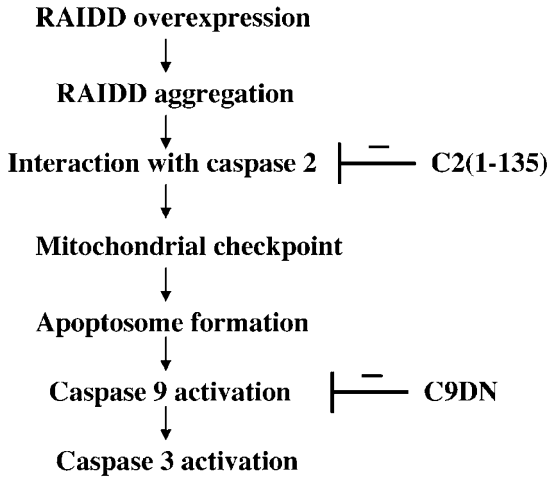

Figure 10 Schematic diagram of RAIDD overexpression-induced death

How could overexpressed RAIDD interact with endogenous caspase 2 in order to begin to activate this pathway in PC12 cells and sympathetic neurons? An unexpected clue has come from our observation that even though two forms of rat RAIDD (RAIDD and RAIDDM) interact to the same extent with the caspase 2 CARD when they are overexpressed in 293T cells (Figure 3b), they have significant differences in their ability to induce death in PC12 cells or sympathetic neurons. The extent of death correlates with the formation of RAIDD aggregates, which are much more frequent with RAIDD, as opposed to RAIDDM, overexpression. Similarly, even though both Flag-tagged human RAIDD (FhRAIDD) and Flag-tagged rat RAIDD (FRAIDD) both may interact with the caspase 2 CARD (27, Figure 3a), only the human form, which forms aggregates in PC12 cells, induces substantial cell death. The difference between these two C-terminal Flag-tagged RAIDD constructs may be related to the divergence of the rat and human isoforms at the C-terminus (see Figure 1a) that, combined with the highly charged nature of the Flag tag, may alter the tertiary structure of RAIDD and its ability to fold upon itself. Truncated forms of rat RAIDD, which fail to induce aggregates, also fail to induce death in PC12 cells or sympathetic neurons. Therefore, in both PC12 cells and sympathetic neurons, there is a direct correlation between the ability of a RAIDD construct to form perinuclear aggregates and to induce cell death (see Table 1). In addition, aggregate-bearing PC12 cells are much more likely to show nuclear and biochemical features of apoptosis compared to cells showing diffuse RAIDD immunostaining or those expressing EGFP, both at baseline and following serum deprivation (see Figures 4, 8 and 9). All these results point to a tight link between RAIDD aggregation and apoptosis.

The correlation between aggregate formation and apoptosis could signify that aggregate formation is the consequence, rather than the cause, of the apoptotic process. However, a number of observations suggest that this is not the case. Many aggregate-bearing cells did not show signs of nuclear apoptosis (see Figure 4a, left panel, Figure 4d, top panel, and Figure 9a; in the latter, in the presence of serum, more than 60% of cells with aggregates were nonapoptotic), indicating that formation of aggregates is an earlier event. When RAIDD overexpression was performed in the presence of BAF, there was a significant increase in the percentage of aggregate-bearing cells, especially in the serum-deprived state, suggesting that cells with aggregates accumulate if apoptosis is inhibited. It appears therefore that aggregate formation precedes apoptosis and, in view of the tight correlation between the two phenomena mentioned above, plays a causative role in the death pathway. We hypothesize that these aggregates enable the recruitment of endogenous caspase 2 in an area of close proximity, leading to caspase 2 activation, similar to what has previously been proposed for the activation of caspase 9 following Apaf-1 oligomerization.[28]

Owing to the potential crucial role of RAIDD aggregate formation in the propagation of apoptosis, we have investigated in more detail the nature of these aggregates. Despite their perinuclear localization, we have found no evidence that they are contained within Golgi, or that they represent aggresomes, as defined by Johnston *et al*.[25] The presence of such aggregates therefore raises a note of caution, and suggests that not all perinuclear inclusion-like structures that are formed following overexpression of certain proteins are aggresomes. These structures may be a reflection of the ability of RAIDD to oligomerize, or may represent complexes of RAIDD with other proteins. Truncated RAIDD constructs, containing part or the full extent of the CARD or the DD, did not form such aggregates. This suggests that both the CARD and the DD of rat RAIDD are required for aggregate formation.

Our data contrast with those previously reported by Shearwin-Whyatt *et al*.[27] In that study, full-length human

Table 1 Summary of the effects of the expression of various RAIDD constructs

	PC12 cells		Sympathetic neurons		SH-SY5Y cells
Construct	**Aggregation**	**Cell death**	**Aggregation**	**Cell death**	**Aggregation**
RAIDD	++	+	++	+	++
RAIDDM	–	±	–	–	NT
FRAIDD	–	±	+	±	–
FRAIDDM	–	NT	NT	NT	–
RAIDD(1–83)	–	–	–	–	NT
RAIDD(1–117)	–	–	–	–	NT
RAIDD(DD)	–	–	–	–	NT
FhRAIDD	++	+	++	NT	++

++, marked effects; +, moderate; ±, variable effects; –, no effect. NT = not tested. Cell death assessments were not performed in SH-SY5Y cells. Note that in every case there is a correlation between the ability of a construct to induce aggregates and to cause death

RAIDD did not induce aggregates, but rather a diffuse distribution of RAIDD, whereas CARD-containing truncated RAIDD formed filaments.[27] In addition to full-length rat RAIDD, we have used the same human RAIDD construct as in that study (FhRAIDD), and have found that in the neuronal cell types we have studied it induces the same perinuclear aggregates as the rat isoform. It is likely that, at least in part, the differences in the results obtained reflect differences in the cell types studied. Our results, showing that full-length RAIDD has the ability to form aggregates in neuronal cells, provide novel insights into the way in which RAIDD may participate in neuronal apoptotic pathways.

A number of other CARD- or death effector domain (DED)-containing proteins have been shown to oligomerize and to form filamentous structures in cells upon overexpression.[27,29,30] In many cases such structures are associated with the induction of cell death.[29] The perinuclear location and the spherical nature of the RAIDD-induced aggregates observed in our study differentiate them from other CARD-induced structures, which have a filamentous, thread-like structure.[27,29,30] Our results indicate an association between the perinuclear aggregates and the death induced by RAIDD. Whether such structures are formed during trophic deprivation-induced apoptosis is not known, but their possible physiological relevance is supported by the findings that RAIDD overexpression acts synergistically with serum deprivation to induce death of PC12 cells, and that the aggregates themselves increase substantially upon trophic deprivation. This increase is even more marked in the presence of BAF, indicating that it is not a consequence of trophic factor deprivation-induced apoptosis, but rather an earlier event, with a possible causal role in this type of death (see Figures 9a and 9b). The fact that BAF did not prevent aggregate formation in the control or serum-deprived state indicates that these aggregates are not dependent on caspase activation for their formation. Thus, if they are formed physiologically during trophic deprivation, this is likely to occur upstream of caspase activation.

In conclusion, we show here that overexpression of RAIDD in PC12 cells and sympathetic neurons induces cell death that is dependent on the caspase 2 CARD and activation of the caspase 9/3 cascade. The formation of RAIDD perinuclear aggregates facilitates apoptosis, likely by bringing caspase 2 molecules in close proximity, leading to their activation. The induction of such RAIDD overexpression-induced aggregates with trophic deprivation and the acceleration of trophic factor deprivation-induced death with RAIDD overexpression suggest that RAIDD, through the formation of aggregates/oligomers, may participate in this apoptotic pathway.

Materials and Methods

Cloning of rat RAIDD/CRADD

We extracted total RNA from PC12 cells using the Trizol reagent and performed RT-PCR (Roche) to generate PC12 cDNA. We then used a nested PCR approach to generate a fragment of rat RAIDD. For the first PCR reaction, we used primers RAIDD51 (5′-GCAGATTAACCAGCTGGC-3′) and RAIDD31 (5′-ACAGCCCGCAGCCCGTTGTG-3′), and for the second one primers RAIDD52 (5′-CTGTCTCTGGGACTGTCCCA-3′) and RAIDD32 (5′-GGAAGGTGGCCTGCTTCCCG-3′). These sequences were selected because they showed a high degree of homology between the published human (Accession #U79115) and mouse (Accession #AJ224738) sequences. The nested PCR reaction resulted in a product of about 130 base pairs (bps), corresponding to bps 506–634 of the human RAIDD sequence. The PCR product was cloned into a TA cloning vector (Invitrogen) and sequenced. Based on the sequence, two primers (RAIDDR5: 5′-AAGGCCAACCATCCCCACAA-3′, and RAIDDR3: 5′-AAAGGCCTCCACCACCTGCGA-3′) were constructed and used for 3′ and 5′ prime RACE (Clontech) respectively, as per the manufacturer's protocol. This resulted in the identification of an upstream initiation ATG site and a downstream stop TGA site matching the ones in human and mouse RAIDD. Based on the identified sequences, we constructed two primers, RAID55 (5′-GACGGAGAAATGGATGCCAGA-3′) and RAIDDF (5′-GGTCTGGTCACTCCAGCATGT-3′), spanning the open-reading frame (ORF) of rat RAIDD, and performed PCR with PC12 cDNA as template ($94^{\circ}C \times 5\,min \times 1$ cycle, $(94^{\circ}C \times 1\,min + 58^{\circ}C \times 1\,min + 72^{\circ}C \times 1\,min) \times 35$ cycles, $72^{\circ}C \times 10\,min \times 1$ cycle). The approximately 600 bp PCR product was cloned into TA and sequenced. For expression studies, rat RAIDD was subcloned into the *Eco*RI site of pCMS-EGFP (Clontech) or pcDNA3 (Invitrogen), and orientation was verified by sequencing.

Other RAIDD constructs

Various RAIDD constructs were generated by PCR, with full-length RAIDD as the template.

Mutant RAIDD (RAIDDM), with a substitution of residue 27 (L27F), was generated by PCR-based site-directed mutagenesis, cloned into TA, and subcloned into the *Eco*RI site of pCMS-EGFP.

C-terminal Flag-tagged versions of RAIDD and RAIDDM were generated by performing PCR with primers RAIDDFlag5 (5′-CGGTCACCATGGATGCCAGAGACAAG-3′) and RAIDDFlag3 (CGGTGACCTCATTTGTCATCATCGTCCTTGTAGTCCATCTCCAGCATGTGCTGGAG-3′), cloning into TA, and subcloning into the *Eco*RI site of pCMS-EGFP.

RAIDD(1–83) (truncated rat RAIDD encompassing residues 1–83) was generated by PCR, using primers RAIDD5myc (5′-TGACGCGTGAAATGGATGCCAGAGAC-3′) and RAIDD53 (5′-AGTCATCTTACCCAGGGAAATTC-3′), and subcloned into the *Mlu*I–*Xba*I sites of a modified pCMS-EGFP vector containing an in-frame Myc sequence upstream of the *Mlu*I site. Another amino-terminal RAIDD construct, RAIDD(1–117), encompassing AA 1–117, was similarly constructed using primers RAIDD5myc and RONup3 (5′-GCTCTAGATCAGTCTGATGGGGAGCTGTT-3′). RAIDD(DD) (truncated rat RAIDD encompassing the DD (residues 115–199)) was generated by PCR, using primers RAIDDT35 (5′-TGACGCGTCCATCAGACCGGCAGATTAACC-3′) and RAIDDF, and similarly subcloned into Myc-containing pCMS-EGFP. Sequencing was performed for all PCR-generated products.

A pCXN2 vector encoding carboxy-terminal Flag-tagged human RAIDD (FhRAIDD, 27) was kindly provided to us by Drs. Sharad Kumar and Shearwin-Whyatt (Adelaide, Australia).

Caspase constructs

C2(1–135), a N-terminal myc-tagged construct encompassing the CARD of caspase 2 (AA 1–135) was generated by PCR, using rat caspase 2 (Stefanis *et al*.[20]) as a template, and primers NEDMyc5 (5′-TGACGCGTAGGATGGCGGCGTCGAGCG-3′) and NEDT3A (5′-TCATGTGCTGGATATCAGAGA-3′). The product was cloned into TA and subcloned into the

*Mlu*I–*Xba*I sites of Myc-containing pCMS-EGFP. C2(1–135M), identical to C2(1–135), except for an AA substitution at residue 57 (L57F), was generated by PCR-based site-directed mutagenesis using external primers NEDMyc5 and NEDT3A and rat caspase 2 as template, and similarly subcloned into Myc-containing pCMS-EGFP. Both constructs were subsequently subcloned into the *Eco*RI–*Xba*I sites of pcDNA3.

Flag-tagged Caspase 9 DN (C327A) in pcDNA3 was generated and subcloned into pCMS-EGFP or pcDNA3 as described previously.[31] In certain experiments we also used a pCMS-EGFP vector encoding Myc-PAI2MT, to control for the effects of overexpression of an additional protein apart from EGFP. PAI2MT is a serpin that lacks the catalytic site, and is therefore not expected to have biological activity and, in particular, to affect the apoptotic pathway. In multiple experiments there was no significant difference between the death induced in PAI2MT/EGFP-expressing cells compared to those expressing EGFP alone. We obtained a pEUK vector encoding PAI-2 from Dr. Philip Bird (Victoria, Australia). PAI2MT, with a mutation at the catalytic site (R380A), was generated by PCR-based site-directed mutagenesis and subcloned into the *Mlu*I–*Not*I sites of the Myc-containing pCMS-EGFP vector.

Cell culture

PC12 cells were grown as described previously,[32,20,22] at 7.5%. CO_2 on rat-tail collagen-coated dishes in RPMI 1640 medium (Life Sciences) containing 1% penicillin/streptomycin (P/S), 5% fetal calf serum (FCS) and 10% heat-inactivated horse serum (HS) (complete medium). In certain experiments PC12 cells were grown on glass coverslips (Carolina Biological Supplies). Sympathetic neuron cultures were derived from sympathetic ganglia of 1- to 2-day-old rat pups.[18,20] Following trypsinization, the ganglia were plated on 24-well collagen-coated dishes, at 0.5–1 ganglia/dish, at 5% CO_2 in RPMI 1640 medium containing 1% P/S, 5% HS and 100 ng/ml human recombinant NGF (generously provided by Genentech), or mouse NGF (Upstate Biotechnology). At 1 day after plating uridine and 5-fluorodeoxyuridine (10 μM each) were added. 293T cells and SH-SY5Y neuroblastoma cells were grown at 5% CO_2 in 100 mm dishes in DMEM (Life Sciences) with 1% P/S and 10% FCS.

Transfection

Transient overexpression of the various genes of interest in PC12 cells or of 293T and SH-SY5Y cells was achieved by Lipofectamine-mediated transfection (Lipofectamine 2000, Life Sciences), following the manufacturer's recommendations. For sympathetic neuron transfection, 3–5 days after plating we combined 3 μg of each DNA in 30 μl of Opti-MEM (Life Sciences) with 4.8 μl of Lipofectamine 2000 (Life Sciences) in 150 μl Opti-MEM. After 1–2 h, we combined the DNA-Lipofectamine mixture with 900 μl of Opti-MEM with 100 ng/ml NGF, and applied the total volume of 1080 μl to six wells in a 24-well dish (180 μl/well). The cultures were left for 4–12 h in this transfection medium, and then this was replaced by the standard RPMI medium.

Trophic deprivation

PC12 cells were mechanically dissociated from 100 mm or 35 mm dishes after five rinses with serum-free RPMI 1640 medium and washed with the same medium 3–4 times by centrifugation and resuspension. PC12 cells were then replated in collagen-coated 24-well or 35 mm dishes.[20,22]

Immunofluorescence

PC12 cells or sympathetic neurons were fixed in freshly prepared 3.7% formaldehyde for 25 min at 4°C, and then incubated with 10% normal goat serum with 0.4% Triton X-100 to block nonspecific binding, followed by incubation with the primary Ab for 1 h at room temperature. Specific antibodies used were: anti-RAIDD (rabbit polyclonal, StressGen AAP-270, 1 : 150), anti-Myc (9E10 mouse monoclonal, derived from a mouse hybridoma cell line, 1 : 1), anti-Flag (mouse monoclonal M2, Sigma, 1 : 400), anti-GM130 (mouse monoclonal, Transduction Laboratories, 1 : 100), anti-active caspase 3 (rabbit polyclonal, Cell Signaling, 1 : 50), anti-cytochrome *c* (mouse monoclonal, Pharmingen, 1 : 500) and anti-γ-tubulin (mouse monoclonal, Sigma, 1 : 400). Following incubation with fluorescent secondary antibodies (Cy2, 1 : 100; or Cy3, 1 : 250, Jackson ImmunoResearch), cells were rinsed in PBS. In some cases, Hoechst 33342 (Sigma, 1 μg/ml) or Yo-Yo (Molecular Probes, 1 : 1500) was added for 20 min at RT, followed by rinses in PBS. The cells were then visualized in an inverted microscope (Leica DM IRB) at $\times$ 40. Pictures were taken on slide film using an Olympus SC35 camera, developed, and scanned on a Sprint 35 scanner operated by Adobe Photoshop. Cells plated on coverslips were placed on glass slides and visualized by confocal microscopy (Zeiss LSM410), or on an upright fluorescence microscope (Zeiss Axioskop 2 Plus) equipped with a digital Spot camera. Identical exposure times were used across conditions.

In certain experiments, in order to examine specifically *in situ* detergent-insoluble components, we incubated the cultures for 10 min in a detergent solution prior to fixation. This buffer contained 85 mM Pipes, pH 6.94, 10 mM EGTA, 1 mM $MgCl_2$, protease inhibitor cocktail (Roche) and 0.1% Triton X-100.[26,33] Following incubation in this buffer, cells were rinsed in PBS and fixed and immunostained as above.

Assessment of cell death

Our first approach for assessing survival/death was to use the pCMS-EGFP vector encoding EGFP and the gene of interest under separate promoters, and count the number of green fluorescent cells over time. However, we discovered that most of the genes of interest were expressed only in a small to moderate proportion of EGFP-fluorescing cells. We have therefore used instead staining with the nuclear dye Hoechst in combination with appropriate immunostaining in order to assess apoptotic cell death in cells that express specific proteins. We counted at least 100 immunopositive PC12 cells or sympathetic neurons per well, in at least three different wells per condition, and evaluated these cells for the presence of the characteristic features of apoptosis: nuclear shrinkage, condensation and clumping. Results are reported as mean $\pm$ S.E.M. Statistical comparisons were carried out using one-way ANOVA with Newman–Keuls *post hoc* comparisons or Student's *t*-test.

Preparation of cell lysates for Western immunoblotting or immunoprecipitation

For generation of crude soluble cell lysates, PC12 cells were rinsed in cold PBS and then collected in buffer A (25 mM HEPES (pH 7.5), 5 mM EDTA, 1 mM EGTA, 5 mM $MgCl_2$, 2 mM DTT, 10 μg/ml each of pepstatin and leupeptin and 1 mM PMSF). The cellular material was left for 20−min on ice and then was sonicated on ice. The lysate was centrifuged for 20 min at 160 000 $\times$ *g*, and the supernatant was used for Western immunoblotting.[20]

To separate lysates into detergent-soluble and -insoluble components, cultures were lysed in a low-detergent buffer containing 0.5% Triton X-100,

25 mM HEPES, 5 mM $MgCl_2$, 1 mM EDTA, 1 mM EGTA and protease inhibitors (Complete, Roche) on ice for 20 min. Detergent-insoluble material was pelleted by ultracentrifugation at 100 000 $\times$ *g* for 30 min and resuspended in SDS SB containing 5% β-mercaptoethanol and boiled for 10 min.

For immunoprecipitation experiments, 293T cells in 100 mm dishes were washed in PBS, and then lysed in RIPA buffer (150 mM NaCl, 1% NP-40, 0.5% deoxycholate, 0.1% SDS, 50 mM Tris, pH 8.0, with protease inhibitors (Complete, Roche)).

Protein concentrations were measured using the Bradford assay (BioRad).

Western immunoblotting

Protein (50–100 μg) was separated by SDS-PAGE (12%, unless specified) and transferred to nitrocellulose membranes. The membranes were blocked in 5% nonfat milk for 1 h at room temperature and probed overnight at 4°C with antibodies raised against RAIDD (1 : 500) or Myc (1 : 10). Protein bands were visualized with horseradish peroxidase-conjugated secondary antibodies (Pierce) and enhanced chemiluminescence (Pierce). To control for protein loading, in certain cases the membranes were stripped and reprobed with mouse anti-β-actin (Sigma, 1 : 20 000).

Immunoprecipitation

We immunoprecipitated 293T cell lysates (1 mg) with 1 μg of anti-Flag monoclonal Ab or with 1 μg of anti-GAPDH (mouse monoclonal, Chemicon) as a negative control. Following preclearing, we incubated the lysates with the antibodies in a rotator for 2 h at 4°C. We then added 30 μl of protein G slurry (Calbiochem) and incubated for an additional 2 h. Pellets were recovered following a quick spin, and washed five times in RIPA buffer. After the last wash, pellets were resuspended in 30–40 μl of SDS SB without β-mercaptoethanol and antigens were eluted by incubation at 85°C for 5 min. Following a quick spin to pellet the beads, the elute was transferred to another tube, and was incubated for 1 h at 37°C, with the addition of β-mercaptoethanol to denature the proteins. Western immunoblotting was then performed as above.

Acknowledgements

This work was supported by a grant from the March of Dimes Foundation (Grant # FY99-318 to LS). Additional support was provided by a Wellcome Burroughs Career Award in Biomedical Sciences (LS), the Lowenstein, Matheson and Parkinson's Disease Foundations (LS), the NIH/NINDS (CMT) and the MDA (CMT). We would like to thank Drs. Lloyd Greene, Michael Shelanski, Isabelle Lang-Rollin and David Park for helpful discussions, Drs. Sharad Kumar and Shearwin-Whyatt for the human RAIDD construct and Dr. Philip Bird for the PAI2 construct.

References

1. Rideout HJ and Stefanis L (2001) Caspase inhibition: a potential therapeutic strategy in neurological diseases. Histol Histopathol 16: 895–908
2. Troy CM and Salvesen GS (2002) Caspases on the brain. J Neurosci Res 69: 145–150
3. Shi Y (2002) Mechanisms of caspase activation and inhibition during apoptosis. Mol Cell 9: 459–470
4. Van de Craen M, Declercq W, Van den brande I, Fiers W and Vandenabeele P (1999) The proteolytic procaspase activation network: an *in vitro* analysis. Cell Death Differ 6: 1117–1124
5. Slee EA, Harte MT, Kluck RM, Wolf BB, Casiano CA, Newmeyer DD, Wang HG, Reed JC, Nicholson DW, Alnemri ES, Green DR and Martin SJ (1999) Ordering the cytochrome *c*-initiated caspase cascade: hierarchical activation of caspases-2, -3, -6, -7, -8, and -10 in a caspase-9-dependent manner. J Cell Biol 144: 281–292
6. Li H, Bergeron L, Cryns V, Pasternack MS, Zhu H, Shi L, Greenberg A and Yuan J (1997) Activation of caspase-2 in apoptosis. J Biol Chem 272: 21010–21017
7. Keramaris E, Stefanis L, MacLaurin J, Harada N, Takaku K, Ishikawa T, Taketo MM, Robertson GS, Nicholson DW, Slack RS and Park DS (2000) Involvement of caspase 3 in apoptotic death of cortical neurons evoked by DNA damage. Mol Cell Neurosci 15: 368–379
8. Duan H and Dixit VM (1997) RAIDD is a new 'death' adaptor molecule. Nature 385: 86–89
9. Ahmad M, Srinivasula SM, Wang L, Talanian RV, Litwack G, Fernandes-Alnemri T and Alnemri ES (1997) CRADD, a novel human apoptotic adaptor molecule for caspase-2, and FasL/tumor necrosis factor receptor-interacting protein RIP. Cancer Res 57: 615–619
10. Koseki T, Inohara N, Chen S and Nunez G (1999) ARC, an inhibitor of apoptosis expressed in skeletal muscle and heart that interacts selectively with caspases. Proc Natl Acad Sci USA 95: 5156–5160
11. Dowds TA and Sabban EL (2001) Endogenous and exogenous ARC in serum withdrawal mediated PC12 cell apoptosis: a new pro-apoptotic role for ARC. Cell Death Differ 8: 640–648
12. Harvey NL, Butt AJ and Kumar S (1997) Functional activation of Nedd2/ICH-1 (caspase-2) is an early process in apoptosis. J Biol Chem 272: 13134–13139
13. Paroni G, Henderson C, Schneider C and Brancolini C (2001) Caspase-2-induced apoptosis is dependent on caspase-9, but its processing during UV- or tumor necrosis factor-dependent cell death requires caspase-3. J Biol Chem 276: 21907–21915
14. Guo Y, Srinivasula SM, Druilhe A, Fernandes-Alnemri T and Alnemri ES (2002) Caspase-2 induces apoptosis by releasing proapoptotic proteins from mitochondria. J Biol Chem 277: 13430–13437
15. Paroni G, Henderson C, Schneider C and Brancolini C (2002) Caspase-2 can trigger cytochrome *C* release and apoptosis from the nucleus. J Biol Chem 277: 15147–15161
16. Lassus P, Opitz-Araya X and Lazebnik Y (2002) Requirement for caspase-2 in stress-induced apoptosis before mitochondrial permeabilization. Science 297: 1352–1354
17. Robertson JD, Enoksson M, Suomela M, Zhivotovsky B and Orrenius S (2002) Caspase-2 acts upstream of mitochondria to promote cytochrome *c* release during etoposide-induced apoptosis. J Biol Chem 277: 29803–29809
18. Troy CM, Stefanis L, Greene LA and Shelanski ML (1997) Nedd2 is required for apoptosis after trophic factor withdrawal, but not superoxide dismutase (SOD1) down-regulation, in sympathetic neurons and PC12 cells. J Neurosci 17: 1911–1918
19. Troy CM, Rabacchi SA, Hohl JB, Angelastro JM, Greene LA and Shelanski ML (2001) Death in the balance: alternative participation of the caspase-2 and -9 pathways in neuronal death induced by nerve growth factor deprivation. J Neurosci 21: 5007–5016
20. Stefanis L, Troy CM, Qi H, Shelanski ML and Greene LA (1998) Caspase-2 (Nedd-2) processing and death of trophic factor-deprived PC12 cells and sympathetic neurons occur independently of caspase-3 (CPP32)-like activity. J Neurosci 18: 9204–9215
21. Haviv R, Lindenboim L, Yuan J and Stein R (1998) Need for caspase-2 in apoptosis of growth-factor-deprived PC12 cells. J Neurosci Res 52: 491–497
22. Stefanis L, Park DS, Yan CYI, Farinelli SE, Troy CM, Shelanski ML and Greene LA (1996) Induction of CPP32-like activity in PC12 cells by withdrawal of trophic support: dissociation from apoptosis. J. Biol. Chem. 271: 30663–30671
23. Chou JJ, Matsuo H, Duan H and Wagner G (1998) Solution structure of the RAIDD CARD and model for CARD/CARD interaction in caspase-2 and caspase-9 recruitment. Cell 94: 171–180

24. Mancini M, Machamer CE, Roy S, Nicholson DW, Thornberry NA, Casciola-Rosen LA and Rosen A (2000) Caspase-2 is localized at the Golgi complex and cleaves golgin-160 during apoptosis. J Cell Biol 149: 603–612
25. Johnston JA, Ward CL and Kopito RR (1998) Aggresomes: a cellular response to misfolded proteins. J Cell Biol 143: 1883–1898
26. Rideout HJ and Stefanis L (2002) Proteasomal inhibition-induced inclusion formation and death in cortical neurons require transcription and ubiquitination. Mol Cell Neurosci 21: 223–238
27. Shearwin-Whyatt LM, Harvey NL and Kumar S (2000) Subcellular localization and CARD-dependent oligomerization of the death adaptor RAIDD. Cell Death Differ 7: 155–165
28. Srinivasula SM, Ahmad M, Fernandes-Alnemri T and Alnemri ES (1998) Autoactivation of procaspase-9 by Apaf-1-mediated oligomerization. Mol Cell 1: 949–957
29. Siegel RM, Martin DA, Zheng L, Ng SY, Bertin J, Cohen J and Lenardo MJ (1998) Death-effector filaments: novel cytoplasmic structures that recruit caspases and trigger apoptosis. J Cell Biol 141: 1243–1253
30. Guiet C and Vito P (2000) Caspase recruitment domain (CARD)-dependent cytoplasmic filaments mediate bcl10-induced NF-κB activation. J Cell Biol 148: 1131–1139
31. Angelastro JM, Moon NY, Liu DX, Yang AS, Greene LA and Franke TF (2001) Characterization of a novel isoform of caspase-9 that inhibits apoptosis. J Biol Chem 276: 12190–12200
32. Greene LA and Tischler AS (1976) Establishment of a noradrenergic clonal line of rat adrenal pheochromocytoma cells which respond to nerve growth factor. Proc Natl Acad Sci USA 73: 2424–2428
33. Cappalletti G, Maggioni MG and Maci R (1999) Influence of MPP+ on the state of tubulin polymerisation in NGF-differentiated PC12 cells. J Neurosci Res 56: 28–35